Research Square

Preprints are preliminary reports that have not undergone peer review.
They should not be considered conclusive, used to inform clinical practice,
or referenced by the media as validated information.

Materialistic characterization, thermal properties, and cytocompatibility investigations on acrylic acid-functionalized nSiO2 reinforced PEEK polymeric nanocomposite

Mugilan Thanigachalam (mugilangct@gmail.com)
Government College of Technology https://orcid.org/0000-0001-5463-8868
Muthusamy Subramanian Aezhisai Vallavi
Durai Sugumar

Research Article

Keywords: Biomaterials, Polymer nanocomposite, In-vitro, Cell adhesion, FESEM

Posted Date: April 14th, 2022

DOI: https://doi.org/10.21203/rs.3.rs-1547282/v1

License: This work is licensed under a Creative Commons Attribution 4.0 International License.
Read Full License

Abstract

Polyether Ether Ketone (PEEK) is a biocompatible alternative to metallic biomaterials because of its unique properties such as relatively low elastic modulus, high mechanical strength, and biocompatibility. A significant issue is that its bioinert feature might lead to implant failure due to poor osseointegration. Therefore, this research aims to develop the $nSiO_2$ ceramic particles reinforced PEEK ($nSiO_2$@PEEK) polymer nanocomposite. The particle size of nanoparticles was measured as 43.6 nm using particle size analyzer (PSA). The fabrication was done by the vertical injection moulding process. The morphology of fabricated composite was analyzed using FESEM. The EDAX and elemental mapping revealed the presence of Si, C, and O elements in $nSiO_2$@PEEK. The structural characteristic of $nSiO_2$@PEEK nanocomposite was investigated using XRD and FTIR. Thermal stability and melting behavior were examined using TGA thermograms and DSC curves. Minimum toxic level (Grade: slight, 1–20%) was observed by in-vitro cytotoxicity assessment using direct and indirect methods. The excellent cell viability was found as 83.6% through MTT assay. The MG-63 cell-adhesion study was conducted subsequently excellent cell growth and cell-morphology were monitored using SEM analysis. Thereby, the developed nanocomposite was found to be good biocompatible properties through this research. Thus it can be suitable as promising biomaterial for medical implant applications.

1. Introduction

PEK and PEEK are thermoplastics with outstanding thermal properties as well as remarkable tensile and compressive strengths. PEEK was invented by the ICI in 1982. There are many industrial and medical uses for the PEEK linear aromatic polymer, and it is also widely considered to be the best thermoplastic material available. PEEK is characterized by its repeating monomers that include two ether and ketone groups. [1]. According to previous studies, PEEK has great potential in dentistry as an additional or alternative material to more conventional metals and ceramics. [2], [3]. PEEK has been used in a variety of dental devices, including dental implants, healing caps, orthodontic braces, and denture prosthetic frames. [4]. The PEEK's enhanced processing capabilities make it an ideal biomaterial for making a patient-specific prosthesis, which might be a significant potential for the biomaterial. Compared to other polymers, the PEEK polymer exhibits excellent fracture resistance [5]. PEEK composite is utilized in clinical dentistry and orthopedic scaffolds because of its excellent strength-to-weight ratio. PEEK composites low bonding energy has been attributed to their chemical inertness and reduced surface energy [6].

There has been a dramatic rise in bone fracture and trauma prevalence across industrialized and developing countries over the past several decades. Because of their osteoconductive, osteoproductive, and osteoinductive qualities, bioactive glasses, particularly those based on silica, are poised to play a critical role in this sector. They found that silica and biosilica-rich microspheres were more effective in stimulating bone regeneration than those made of polylactide-co-glycolic acid (PLGA). Using silica- and biosilica-containing microspheres to replace natural bone tissue has been suggested.

In-vitro measurements of CCK-8 cell cytotoxicity and qualitative comparisons of inverted fluorescence microscopy images of cell morphology showed that adding Al_2O_3 decreased the cell survival of PEEK slightly. A particular surface topography (defined roughness equal to approx. Ra = 0.30 m), which provides the best potential survivability of human osteoblasts, was found in 30 nm Al_2O_3 reinforced composites. There is evidence that current glass-reinforced PEEK or Ti-6Al-4V manufactured using fast prototyping technology can be utilized to construct implants that can be used in clinical situations [7]. PEEK implants may be improved in cytocompatibility, soft tissue integration, and osseointegration by using TiO_2 nanostructure forms [8].

The 30 wt % HA/PEEK composite was selected in the cytotoxicity experiments. Alkaline phosphatase (ALP) activity was shown to be greater in PEEK composite samples than in UHMWPE and pure PEEK, as evidenced in the cell assays. After seven days of immersion in SBF, the HA/PEEK composite was covered with apatite growth, which continued to grow over extended periods. In animal experiments, there was higher bone contact and bone growth around the HA/PEEK (HA-Hydraxyapatide) composite than around UHMWPE or pure PEEK [9]. The PEEK and CFR-PEEK (CFR- Carbon Fibre Reinforcemnt), were machined and injection moulded, as well as polished (Ra = 0.200microm) and rough (Ra = 0.554microm) cpTi, were all considered. On PEEK (Ra = 0.095microm) and CFR-PEEK (Ra = 0.350microm) injection moulded versions, osteoblast adhesion at 4 hrs was equivalent to titanium. Both PEEK and CFR-PEEK materials were much less machined than their natural counterparts (Ra = 0.902microm and 1.106microm) and determined at 48 hrs. As a result, the maximum thymidine incorporation was found in the injection moulded unfilled PEEK, which was much greater than the rough titanium control [10]. When applied to the PEEK disc implant, the HA coating adhered strongly and formed a homogeneous layer that was simple to clean. Cell adhesion and viability were both increased in early cell adhesion and viability tests performed on the material. It was shown that cells grown on HA-coated PEEK discs had increased ALP activity and calcium concentration, and that they had a higher calcium concentration. The expression of osteoblast development indicators such as ALP, bone sialoprotein, and runt-related transcription factor was also increased in these cells [11], as well as the expression of other genes. The mesenchymal stem cell proliferation experiment results revealed that the treated layer had more significant cell proliferation when comparing treated and untreated PEEK. The apatite formation data revealed the presence of HA growth on the treated PEEK. However, there was no evidence of HA development on the untreated PEEK even after two weeks of testing [12].

The success or failure of implants is primarily determined by their ability to integrate with the surrounding bone, which is a significant function of their biocompatibility with the surrounding bone. As a result, nanoparticles of metal oxides have lately become widely employed in composites to improve the topographical and biological characteristics of the materials.

Therefore, the present research aims to develop the functionalized ceramic nanoparticle reinforced PEEK polymer nanocomposite. The acrylic acid-functionalized $nSiO_2$ particles were used as reinforcement and PEEK as a matrix material. The composite was fabricated through the vertical injection moulding process. The morphology of the developed composite sample was investigated using Field Emission

Scanning Electron Microscope (FESEM) analysis. The various elements present in the fabricated composite were analyzed using Energy Dispersive X-Ray Analysis (EDAX) and the elemental mapping technique. The material was further characterized with the help of X-ray Diffraction (XRD), Fourier-Transform Infrared Spectroscopy (FTIR), Thermal Gravimetric Analysis (TGA), and Differential Scanning Calorimetry (DSC) analysis. The biocompatibility of the newly developed nanocomposite has been investigated through the invitro direct and indirect cytotoxicity investigations. Cell viability and cell adhesion studies were carried out to confirm biocompatibility. The MG-63 cell adhesion was investigated using SEM micrographs.

2. Material And Methodology

2.1 PEEK and $nSiO_2$

The PEEK polymer is utilized as a matrix material to develop the polymer nanocomposite. The melting point temperature of PEEK is around 343°C and was purchased from Engineered Polymers Ind Pt Ltd. The ceramic $nSiO_2$ was purchased from AD Nano Technologies Pvt Ltd., Karnataka, India. It was selected for incorporation into the polymer matrix as reinforcement, and the melting point of $nSiO_2$ is about 1710°C. The flow diagram of the methodology of the current research work is shown in Fig. 1.

The ceramic $nSiO_2$ nanoparticles were used in the functionalization process (using acrylic acid) [13]–[15]. The $nSiO_2$ particles were combined with 30 grams of acrylic acid. It was incorporated into a second mixture, which contains 32 grams of a diluted hexane solution of water, and successfully mixed. The produced mixture was sonicated for 20 minutes at room temperature using an ultra probe sonicator, after which they were allowed to cool to room temperature. Centrifugation at 13,000 rpm for up to 2 hours was used to remove adsorbed residues that had collected during the functionalization process. The functionalized nanoparticles were obtained by drying the $nSiO_2$ particles under a vacuum.

2.2 Particle size analyser

To determine the particle size of functionalized $nSiO_2$, the ZETASIZE NANO Zs90 type PSA was used at a constant temperature of 25°C. The $nSiO_2$ particles sample refractive index and absorption values are 2.5 and 0.1, respectively. The dispersant used in PSA is water with a refractive index of 1.330.

2.3 Fabrication of nanocomposite using injection moulding

A vertical plastic injection moulding procedure was used to fabricate a functionalized ceramic nSiO2 particle reinforced PEEK polymer nanocomposite. The ratio of 10:1.2 weight percentage was selected to develop the $nSiO_2$@PEEK polymer nanocomposite. The PEEK polymer was combined with preheated $nSiO_2$ particles in the proper ratio before being fed into the moulding machine. As a result of this, the PEEK polymer was blended with the nanoparticles at between 90 and 100°C. Due to melt blending phenominum inside the chamber, the reinforcement was mixed with the PEEK matrix. The semi-pressurized blended PEEK matrix and ceramic reinforcement were injected into the die cavity are injected

and the pressure maintained in the machine was around 45–50 bar. Then the die was opened, and the composite specimens were separated.

2.4 FESEM and EDAX analysis

FESEM was used to examine the surface morphological characteristics of the fabricated $nSiO_2$@PEEK nanocomposite specimen. The elemental composition of the developed $nSiO_2$@PEEK was also determined using energy dispersive X-ray analysis (EDAX), which allowed to validate of the existence of elements in the injection moulded specimen.

2.5 FTIR

When the $nSiO_2$@PEEK polymer nanocomposite sample was examined using the FTIR method, it was discovered that it included both organic and inorganic components. The infrared absorption frequency range 400–4000 cm^{-1} was used to identify the actual functional groups contained in the sample, which was calculated using spectrum data collected by the automated spectroscopy software. The incident laser of 1 mW with a resolution of 4 cm-1 was used to record spectra in order to improve the signal-to-noise ratios.

2.6 XRD

X-ray diffractometry (XRD) is a technique used to identify the underlying crystal structure of a material; it allows for the verification of the crystallinity and structure of the nSiO2@PEEK polymer nanocomposite sample. The fitting of XRD patterns was used to calculate the lattice parameters. The XRD analysis was carried out using Rigaku Corporations, MiniFlex model machine with the 2 range from 10° to 90°. The XRD patterns of concrete specimens are identified using a standard database (the JCPDS database) for XRD patterns, which contains information on a wide range of crystalline phases.

3. Thermal Properties

3.1 Thermal stability by TGA and melting behavior by DSC

TGA is a technique for determining the thermal stability of materials, particularly polymers. The developed polymer nanocomposite sample was heated in an air environment under a nitrogen atmosphere from 50°C to 500°C at a rate of 20°C/min. The data on thermal behavior was gathered through the use of the setup program. Experiments were conducted on samples with an average mass of 20 mg and a purge gas flow rate of 20 mL/min, with the samples being weighed before each experiment. In this approach, changes in the weight of a specimen are measured while the temperature of the specimen is being raised over time. TGA is also used to determine the moisture and volatile contents of a sample.

The DSC analysis determines the amount of energy required to raise the sample's temperature compared to the reference material. The sample and reference material temperatures are kept almost constant, with

the heat flux generated during the analysis making up the difference. DSC experiments were conducted on polymer nanocomposite sample on a NETZSCH model, 1100M with Q50 type thermobalance under a nitrogen atmosphere. A sample with an average mass of 10 mg was heated from 10°C to 500°C at a rate of 20°C/min.

4. Biocompatible Assessment

4.1 MG-63 cell line and cell culture

The MG-63 cell line was used for in vitro studies, obtained from the National Centre for Cell Science (NCCS) in Pune, India. The cell line is human, has bone origins, and has the shape of osteosarcoma. An established and well-characterized cell line, MG-63, can produce consistent findings. Fetal bovine serum was added to a minimum essential medium to create a cell culture medium. As an appropriate serum, it has more growth factors that may be used in several uses for cell culture since it has the lowest level of antibodies in the market [16].

4.2 In-vitro direct and indirect cytotoxicity assay

The Ethylene Oxide (ETO) sterilization is used to sterilize the specimens to test for in-vitro cytotoxicity. For a pressure 5 bar and a temperature of 50°C, the samples were first preconditioned for 20–30 minutes and then humidified for another 20–30 minutes. The sample was exposed to 100% ETO dose for the next seven hours, followed by aeration for the next twelve hours [17]. Finally, an ETO sterilized sample was prepared and used. The experiments were conducted at South India Textile Research Association (SITRA, Coimbatore, India). For in-vitro direct and indirect cytotoxicity, ISO 10993:5 standard was followed [18]. The percentage of cytotoxic effect was calculated by using the following Eq. (1).

$$Cytotoxicreactivity(\%) = \left\{\frac{Control - treated}{Control}\right\} \times 100$$

1

4.3 Cell viability assay

Cells derived from human osteosarcoma (MG-63 osteoblast-like cells) were cultured in a standard culture medium at 37°C, the cultures were kept in a humidified environment with 5% CO_2 that was replaced every two days. The mitochondrial dehydrogenase activity was used to measure the proliferation and viability of cells colonizing the samples using MTT assay. MG-63 cells were planted in well plates with 5% CO_2 to examine the $nSiO_2$@PEEK polymer composite sample's cytotoxicity. Then it was placed for 4 hours at 37°C with MTT solution on top of the well in a 1ml serum-free medium. The plate was shaken for 15 minutes after removing the solution before the absorbance was measured with an ELISA microplate reader. The percentage of viable cells was then calculated with control [19]–[21]. The cell viability was calculated by using Eq. (2).

$$ViabilityofMG-63cells(\%) = \left\{\frac{Treated}{Control}\right\} \times 100 (2)$$

4.4 Cell adhesion study

The cell adhesion experiment was performed on a functionalized ceramic $nSiO_2$ reinforced PEEK polymer nanocomposite. An autoclave was used to sterilize a piece of composite material, after which cells were grown on it. The seeded test sample was cultivated in the same CO_2 incubator as the control sample under identical circumstances. After two days into the experiment, the culture media had to be replaced and the wells were cleaned out. Phosphate buffer saline was used to wash the samples twice to eliminate any leftover pollutants after the prescribed time period (48 hours) (pH 7.4). MG-63 cells attached to the samples were dehydrated twice for a total of 10 minutes each time, with a succession of ethanol/water combinations used in each step [22]. The cells were fixed for an hour at room temperature in a glutaraldehyde solution of 2% before being dehydrated for 10 minutes at a time using a succession of ethanol/water solutions. To keep the cells in each well in their original shape, hexamethyldisilazane (0.5 mL) was applied to each well next [20], [23]. The samples were prepared for scanning electron microscopy using gold sputtering before being analyzed.

5. Results And Discussion

5.1 Particle size analysis

The Purchased $nSiO_2$ powder was introduced into functionalization through acrylic acid to improve properties and enhance bio integration of material to the human system. The functionalized $nSiO_2$ particle size is analyzed using the particle size analyzer and obtained the average particle size about 43.6 nm. The histogram shown in Fig. 2 gives the binomial lognormal distribution of particle sizes.

5.2 FESEM morphology analysis

The presence and distribution phenomena of $nSiO_2$ reinforcement on the polymer matrix were observed using FESEM morphological analysis. Figure 3(a) reveals the proper distribution of nanoparticles with the matrix. Also, the functionalized nanoparticles were thoroughly combined with the PEEK matrix was observed due to the acrylic acid functionalization. And also confirms the proper mixing of nanoparticles with the PEEK matrix during the plastic injection moulding process. In a few regions, the agglomeration of nanoparticles was also observed due to covalent bond formation [24]. The region of agglomeration is shown in Fig. 3(b). The suitable temperature helps to bind the nanoparticles with PEEK completely, which is clearly observed from the FESEM analysis. The presence of $nSiO_2$ particles in the developed nanocomposites was focused with the help of the cross-sectioned specimen's FESEM image shown in Fig. 3(c). From the above observations, the interfacial force between the functionalized $nSiO_2$ particles with the PEEK matrix promoted the uniform dispersion of nanoparticles in the developed $nSiO_2$@PEEK polymer nanocomposite.

5.3 EDAX and elemental mapping

The element presence and the confirmation were investigated through the EDAX and elemental mapping technique. The presence of $nSiO_2$ particle was confirmed with the help of EDAX spectrum results are shown in Fig. 4(a). From the EDAX analysis, the elements like carbon (C), oxygen (O), and Silica (Si) were identified. The weight percentage of C, O, and Si elements are 68.54%, 19.32%, and 12.14%, respectively. The atomic percentages of C, O, and Si elements are observed as 77.68%, 16.42%, and 5.89%, respectively. The elemental mapping was carried out to verify the dispersion of elements on the surface of the developed nanocomposite, which is shown in Fig. 4(b, c). Various colours were used to record the specific elemental mappings for each element as shown in Fig. 4(d, e, and f).

5.4 FTIR

FTIR analysis is an effective technique that is sensitive to interfacial interaction, intermolecular interaction, etc. order to identify the presence of polymer & filler, monitor the absorption peak shifts and interfacial interactions in a specific region to determine the functional groups interaction related to the PEEK, $nSiO_2$. FTIR spectra of $nSiO_2$@PEEK polymer composite were taken from 400 cm^{-1} to 4000 cm^{-1} and shown in Fig. 5. The spectrum shows carbonyl group (C = O) stretching at 1759 cm^{-1}, which is the important characteristic of the ketone bond for PEEK [25]. The sharp peaks were observed at 3692 cm^{-1} and 1496 cm^{-1}, confirming the strong O-H stretch functional group. The presence of SiO_2 was confirmed with the help of the Si-O-Si group at 981 cm^{-1} and Si-O at 504 cm^{-1} [26]in the FTIR spectra. The ether functional group (R-O-R) was identified at 1209 cm^{-1} wavenumber [27], which supports confirming the PEEK in the FTIR spectra of $nSiO_2$@PEEK polymer composite.

5.5 XRD

The phase structure and crystallinity of the developed $nSiO_2$@PEEK polymer composite were investigated by XRD pattern, as shown in Fig. 6. The Sharp prominent peak revealed the presence of PEEK in the $nSiO_2$@PEEK polymer composite, which was indicated by a green color symbol. The sharp and minor fine peaks in the XRD pattern of $nSiO_2$@PEEK polymer composite indicated the presence of crystalline $nSiO_2$. The broad peak of PEEK signified the amorphous nature of the PEEK phase. Based on the XRD pattern, the diffraction peaks were observed at 18.53°, 22.35°, and 24.52°, which indicates the presence of PEEK with lattice parameters (hkl) are (110), (110), and (200) respectively. The presence of $nSiO_2$ was confirmed with the help of peaks observed at 42.32°, 5.49°, and 63.76° with (201), (210), and (212) planes. The observed broader peak in the XRD pattern pronounced the more significant amount of amorphous polymer compound present in the nanocomposite matrix.

5.6 TGA and DSC

The TGA thermogram of $nSiO_2$@PEEK polymer composite is shown in Fig. 7. This analysis was carried out to investigate the change in mass loss of the sample concerning temperature changes under the nitrogen gas condition. According to the TGA thermogram, the developed composite sample showed

three degradation stages. In the first thermal degradation stage, the volatile components like moisture of the material were lost, and at the end of the first stage, 2.67% of mass loss was observed. In the second stage of the thermal degradation, the mass loss was monitored at about 3.87% between 93.65°C to 209.32°C. This is due to the decomposition of the organic component present in the composite sample. Further thermal decomposition was monitored between 209.32°C to 452.17°C. The mass loss was found as 4.48% due to the decomposition of a few carbon residuals. The total mass loss was found as 11.02% in the TGA analysis, which shows the developed nanocomposite's relatively higher thermal stability.

DSC was adopted to investigate the influence of $nSiO_2$ on the crystallization and melting behavior of PEEK in the developed nanocomposite. The DSC curve of $nSiO_2$@PEEK polymer composite was observed and depicted in Fig. 6. The crystallization temperature of net PEEK was about 310°C. Interestingly, the reinforcement of $nSiO_2$ leads to a slight improvement in melting temperature, which confirms the thermal stability of $nSiO_2$@PEEK polymer composite. The peak melt temperature was monitored as 341.13°C, and the melt onset temperature was 342.72°C. The nanoparticle loaded with PEEK signified the higher thermal stability up to the temperature of 348.56°C. The energy observed during the functionalized nSiO2 reinforced PEEK polymer composite analysis was about − 13.72 J/g. This energy absorption was happened due to the endothermal reaction of the sample in heating conditions. The further increasing the temperature, the composite reached the amorphous state.

5.7 Direct cytotoxicity assessment

The composite sample was sterilized with ETO under PBS incubation condition at 37 ± 1°C for 24 hrs duration. The cultured MG-63 line cell line was replaced with a new fresh medium. The liquid extract of the developed nanocomposite sample was introduced into cell culture. Then the MTT assay was added in all the wells, and the incubation of 4 hrs was conducted. After that minimum amount of organic sulfur and dimethyl sulfoxide was added to the wells. Finally, the cytotoxicity assessment results of three replicates were observed with the help of a photometer. The percentage of cytotoxic effect was calculated by using the following Eq. (1).

The cytotoxicity percentage was found as 16.4%, shown in Fig. 9. It was compared in the standard reactivity level reference table [16]. The grade was assigned as slight cytotoxic reactivity between the cytotoxicity level of 1–20%. The inverted phase-contrast microscopic images of control and sample dishes were monitored, as shown in Fig. 9(a, b). From this observation, the living and nonliving cells were identified to measure the cytotoxic effect of the composite sample. The maximum number of living cells was addressed through this assessment. Thus the minimum toxic level was confirmed to the developed nanocomposite material.

5.8 Indirect Cytotoxicity assessment

The MG-63 cell culture was prepared after 48 hrs culture period, and then the cells have interacted with the specimen using an *in-vitro* indirect method of cytotoxicity evaluation. Further 24 hrs, the grade of cytotoxic reactivity was measured and compared with the standard reference table [18]. The viable and

nonviable cells were monitored using microscopic image observations. The viable (living) and nonviable (nonliving) cells are shown in Fig. 10, with different color dotted circles. From this observation, the maximum number of viable MG-63 cells were noticed in the test culture, which has been interacted with the developed composite specimen. The level of cytotoxicity fell between grade 2 (slight reactivity level) during the measurement of cytotoxicity by indirect method. This reactivity level was lying in an acceptable range while deciding the material as biocompatible one for medical applications.

5.9 Cell viability assay

The biocompatibility of $nSiO_2$@PEEK polymer composite in MG-63 type cells was evaluated using the MTT test assay method. The composite sample was subjected to MG-63 cells that were cultured for 48 hrs. After interaction with the cell line, the cell viability was calculated by using Eq. (2). The cell viability of the developed $nSiO_2$@PEEK composite was achieved as 83.6% from the MTT test assay, as shown in Fig. 11. This is due to the surface functionalization of nanoparticle reinforcement into the PEEK matrix. The addition of $nSiO_2$ influenced the viability and growth of cells in the assessment. Therefore, functionalized $nSiO_2$ in PEEK polymer nanocomposite promotes good cell viability. Thus, it was confirmed that developed composite material could be a suitable candidate for medical implant application with excellent biocompatibility.

$$ViabilityofMG-63cells(\%) = \left\{\frac{Treated}{Control}\right\} \times 100 \quad (2)$$

5.10 Cell adhesion study

The cell adhesion study has been conducted after confirmation of the good cytotoxicity and excellent cell viability through in-vitro direct, indirect cytotoxicity assessment and cell viability tests. In this study, the MG-63 cell morphologies and adhesion of cells growth have been observed through the SEM analysis. After proper sterilization of composite samples by autoclave, the seven days growth MG-63 cells were attached to the surface of the composite samples. Gold sputtered cells attached samples were undergone the SEM investigation to get the morphological details of MG-63 cells on the surface. Also, the cell growth and proliferation of adhered cells were monitored using SEM observations. The polygon shape MG-63 cells [28]and spindle shape cell morphologies were identified in Fig. 12 (a-c). The filopodia shape [29] was identified clearly and confirmed the excellent MG-63 growth, as shown in figure (d-f). The observed hairline structure spread throughout the entire surface of the sample helped to confirm the growth of living cells on the composite surface. These confirmations reveal the excellent osteointegration of cell-implant interaction. Thus, the addition of $nSiO_2$ greatly signified the biological reaction of the cell enhancement to the cell adhesion samples. Hence, it has been proven that the developed $nSiO_2$@PEEK nanocomposite has good cytocompatibility.

6. Conclusion

The outcomes of the present research work are as follows. To overcome the short comes of the metal implants, the functionalized ceramic $nSiO_2$ reinforced polymer nanocomposite was developed using an injection moulding process. The uniform distribution and presence of $nSiO_2$ particles in the fabricated composite were investigated using FESEM morphologies and EDAX analysis. The presence of functional groups and crystallinity conditions have been analyzed by FTIR and XRD respectively. The improved thermal stability of the $nSiO_2$@PEEK composite was found due to the addition of $nSiO_2$ particles. The melting behavior of the composite was improved up to 348.56°C, which was monitored using DSC analysis. The *in-vitro* cytotoxicity evaluations reveal the excellent biocompatibility of the polymer nanocomposite material. The grade 1 (slight: minimum toxic level) cytotoxic reactivity level (16.4%) has been achieved from both direct and indirect cytotoxicity assessments. The filopodia shape of MG-63 cells were identified through the cell adhesion study, which confirms the excellent cell growth on the developed $nSiO_2$@PEEK polymer nanocomposite. Thus, the above results confirmed that the developed composite could be a promising alternative for metal dental implants.

References

1. R.D. Babu, P. Prakash, D. Devaprakasam, Trends Biomater. Artif. Organs **31**(4), 164 (2017)
2. C. Liao, Y. Li, S.C. Tjong, Polym. (Basel) **12**(12), 1–48 (2020). doi:10.3390/polym12122858
3. S. Mishra, R. Chowdhary, Clin. Implant Dent. Relat. Res. **21**(1), 208 (2018)
4. S. Najeeb, Z. Khurshid, S. Zohaib, M.S. Zafar, J. Oral Implantol **42**(6), 512 (2016). doi:10.1563/aaid-joi-D-16-00072
5. G. LESIUK, A. SAWICKA, J. CORREIA, R. FRĄTCZAK, Eng. Struct. Technol. **9**(4), 207 (2017). doi:10.3846/2029882x.2017.1417062
6. T. Shimizu, S. Fujibayashi, S. Yamaguchi, K. Yamamoto, B. Otsuki, M. Takemoto, M. Tsukanaka, T. Kizuki, T. Matsushita, T. Kokubo, S. Matsuda, Acta Biomater. **35**, 305 (2016). doi:10.1016/j.actbio.2016.02.007
7. P. Olesik, M. Godzierz, M. Kozioł, J. Jała, U. Szeluga, J. Myalski, Mater. (Basel) **14**(14), 10 (2020). doi:10.3390/ma14144024
8. X. Gu, X. Sun, Y. Sun, J. Wang, Y. Liu, K. Yu, Y. Wang, Y. Zhou, Front. Bioeng. Biotechnol. **8**(1), 1508 (2021). doi:10.3389/fbioe.2020.631616
9. J. Geringer, W. Tatkiewicz, G. Rouchouse, Wear **271**(12), 2793 (2011). doi:10.1016/j.wear.2011.05.034
10. K.B. Sagomonyants, M.L. Jarman-Smith, J.N. Devine, M.S. Aronow, G.A. Gronowicz, Biomaterials **29**(11), 1563 (2007). doi:10.1016/j.biomaterials.2007.12.001
11. B. Cecen, D. Kozaci, M. Yuksel, D. Erdemli, A. Bagriyanik, H. Havitcioglu, J. Appl. Biomater. Funct. Mater. **13**(1), 10 (2015). doi:10.5301/jabfm.5000182
12. D. Almasi, W.J. Lau, S. Rasaee, R. Sharifi, H.R. Mozaffari, Prog Biomater. **9**(1), 35 (2020). doi:10.1007/s40204-020-00130-7

13. D. Masoud, G. Matineh, Z. Ali, M. Reza, Z.B. Taraghdari, A. Milad, E.N. Zare, A. Tarun, V.V. Padil, M. Babak, F. Rossi, Prosthesis **2**(2), 117 (2020). doi:10.3390/prosthesis2020012
14. S. Chen, J. Yang, K. Li, B. Lu, L. Ren, Int. J. Food Prop. **21**(1), 2557 (2018). doi:10.1080/10942912.2018.1534125
15. S. Siva, G. Raju, Srinivasa Rao, C. Samantra, Meas. J. Int. Meas. Confed **140**, 254 (2019). doi:10.1016/j.measurement.2019.04.004
16. C.B. Ayyanar, K. Marimuthu, B. Gayathri, Sankarrajan, Polym. Polym. Compos., 2020, 29(9). doi:10.1177/0967391120981551
17. M. Thanigachalam, A.V. Muthusamy Subramanian, Polym. Technol. Mater. **61**(5), 566 (2021). doi:10.1080/25740881.2021.2005093
18. C. Balaji Ayyanar, K. Marimuthu, Polym. Polym. Compos. **28**(4), 285 (2020). doi:10.1177/0967391119872877
19. M.A. Malvindi, V. Brunetti, G. Vecchio, A. Galeone, R. Cingolani, P.P. Pompa, Nanoscale **4**(2), 486 (2012). doi:10.1039/c1nr11269d
20. B. Zheng, H. Xu, L. Guo, X. Yu, J. Ji, C. Ying, Y. Chen, P. Shen, H. Han, C. Huang, S. Zhang, ACS Sustain. Chem. Eng. **5**(10), 9126 (2017). doi:10.1021/acssuschemeng.7b02051
21. R. Bengalli, S. Ortelli, M. Blosi, A. Costa, P. Mantecca, L. Fiandra, Nanomaterials, 2019, 9(7). doi:10.3390/nano9071041
22. M. Thanigachalam, A.V. Muthusamy Subramanian, J. Biomater. Sci. Polym. Ed., 2021, doi:10.1080/09205063.2021.2014028
23. J. Venkatesan, S. Anil, Biotechnol. Bioprocess. Eng. **26**(3), 312 (2021). doi:10.1007/s12257-020-0359-0
24. G. Shi, Z. Cao, X. Yan, Q. Wang, Mater. Chem. Phys. **236**(3), 121778 (2019). doi:10.1016/j.matchemphys.2019.121778
25. B. Liu, W. Hu, G.P. Robertson, M.D. Guiver, J. Mater. Chem. **18**(39), 4675 (2008). doi:10.1039/b806690f
26. D.R. Eddy, S.N. Ishmah, M.D. Permana, M. Lutfi Firdaus, Catalysts **10**(11), 11 (2020). doi:10.3390/catal10111248
27. M. Kumar, E. Gnansounou, I.S. Thakur, Environ. Technol. Innov. **18**, 100647 (2020). doi:10.1016/j.eti.2020.100647
28. B. Sarker, R. Singh, R. Silva, J.A. Roether, J. Kaschta, R. Detsch, D.W. Schubert, I. Cicha, A.R. Boccaccini, PLoS One **9**(9), 107952 (2014). doi:10.1371/journal.pone.0107952
29. L. Chen, J. Hu, J. Ran, X. Shen, H. Tong, Poly Compos. **37**(1), 81 (2016)

Figures

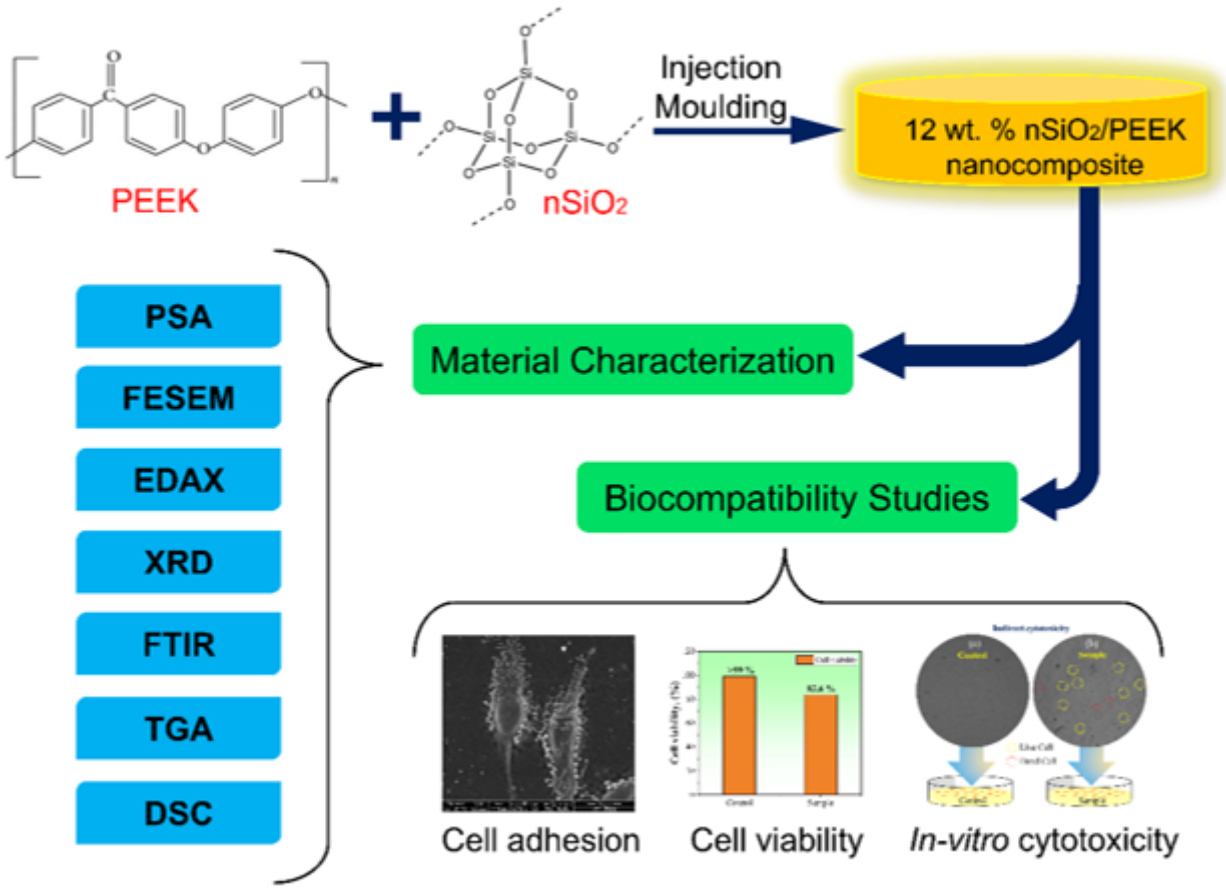

Figure 1

Schematic flow diagram of a methodology of the current research work

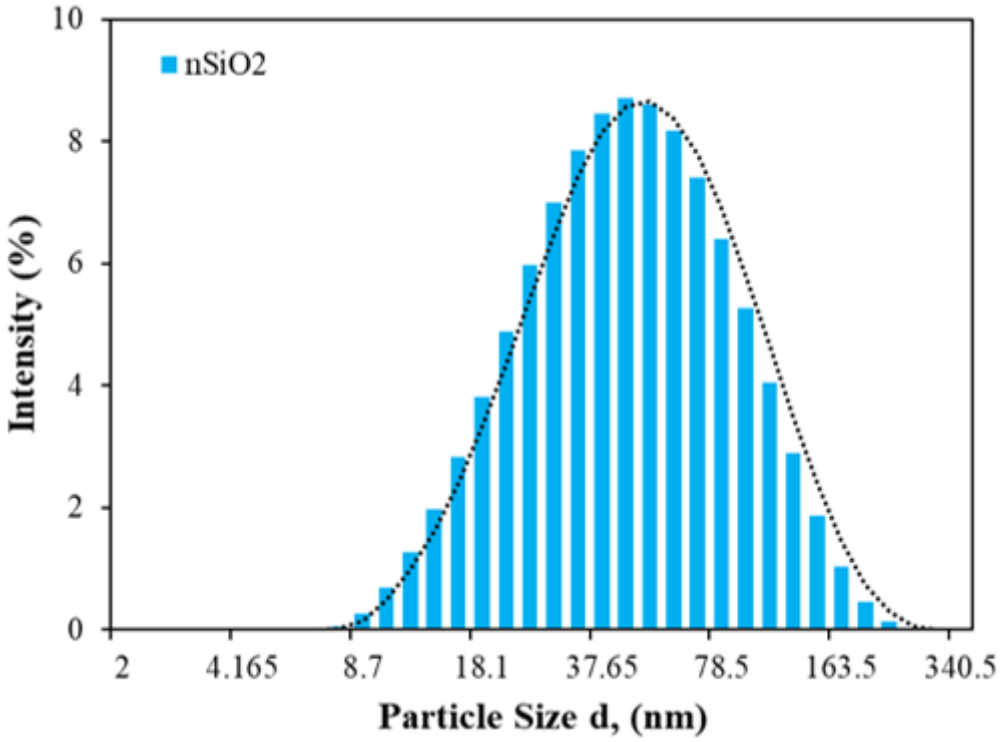

Figure 2

Histogram analysis of particle size distribution

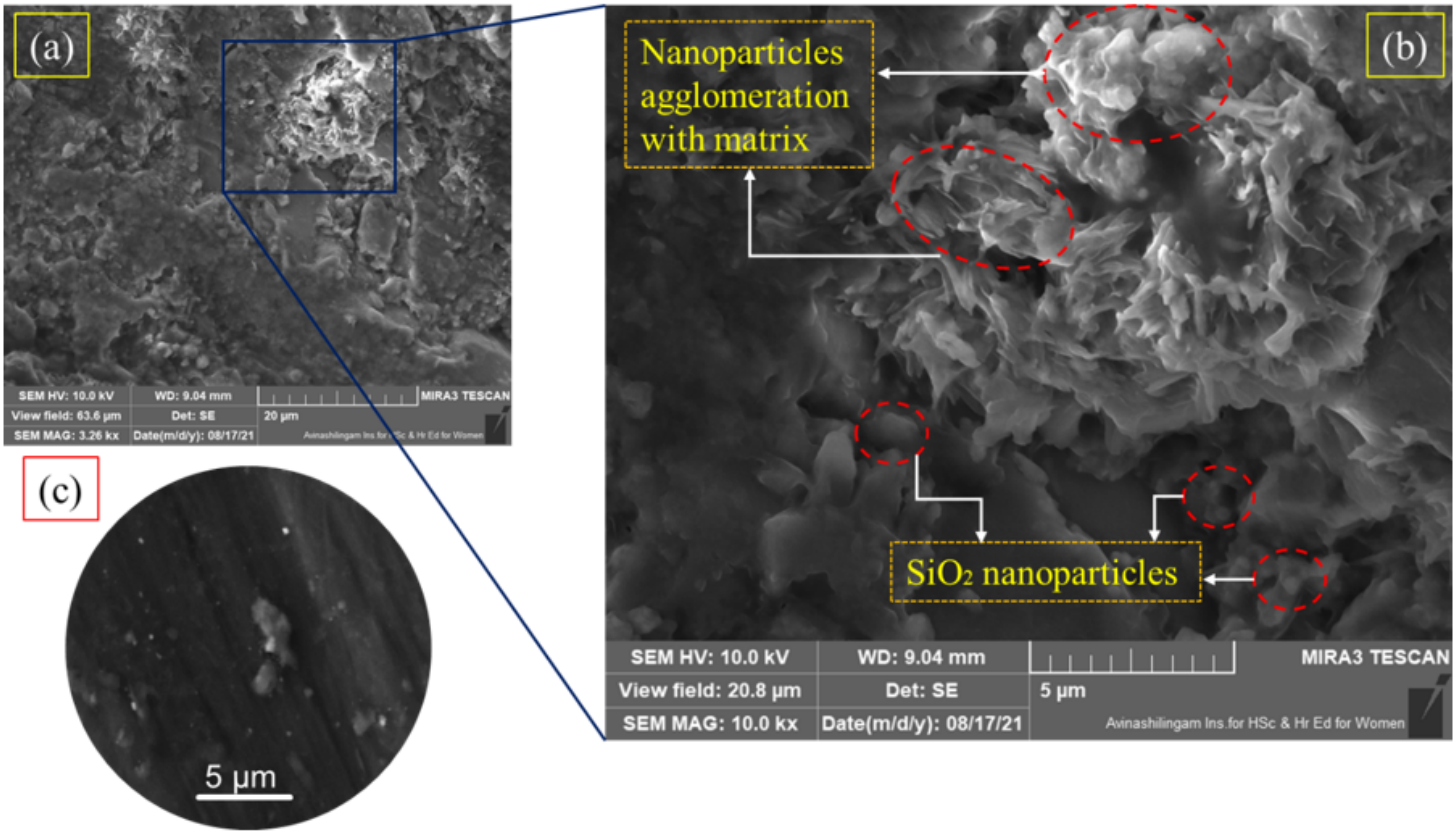

Figure 3

FE-SEM morphologies of $nSiO_2$@PEEK polymer composite (a-c).

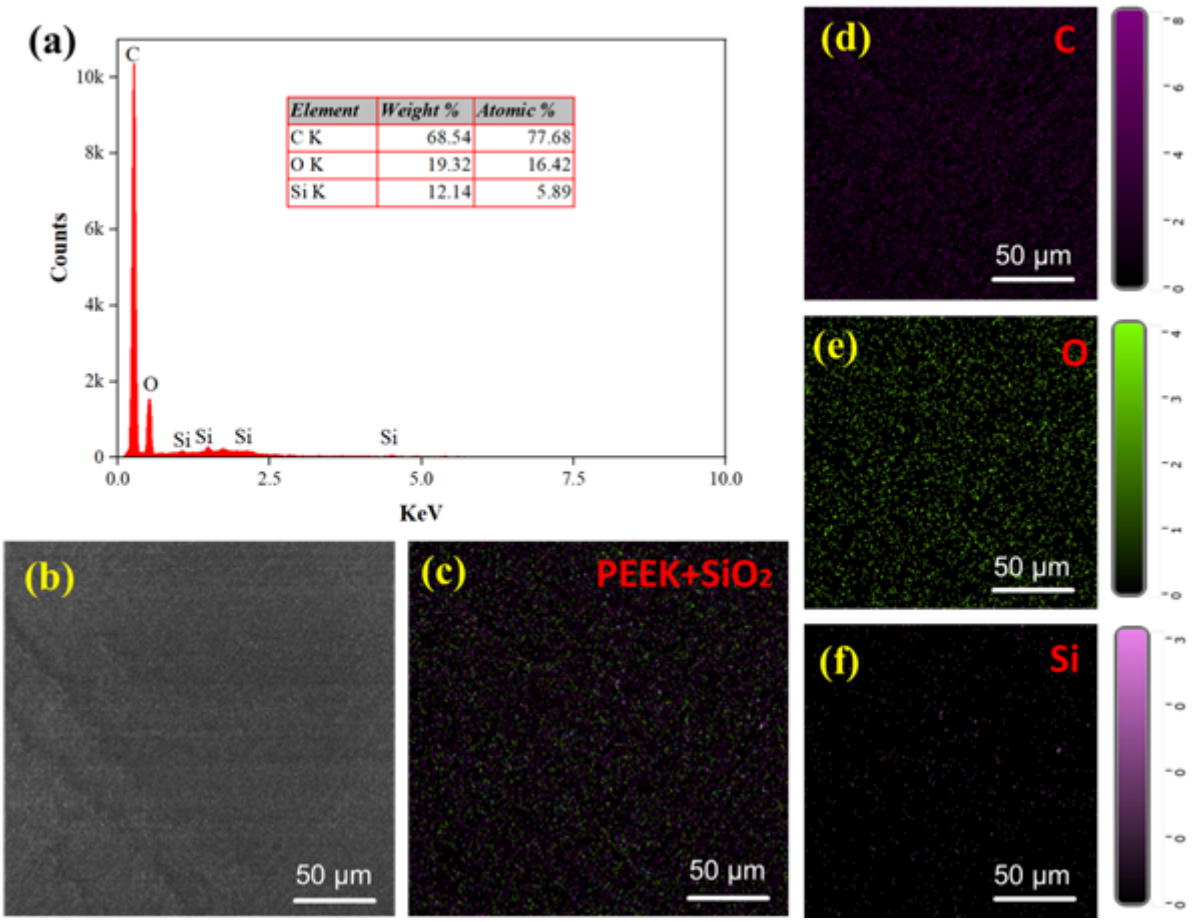

Figure 4

(a) EDAX spectrum of $nSiO_2$@PEEK polymer composite, (b) EDAX analysed region and (c-f) elemental mappings for $nSiO_2$@PEEK polymer composite, C, O, Si elements.

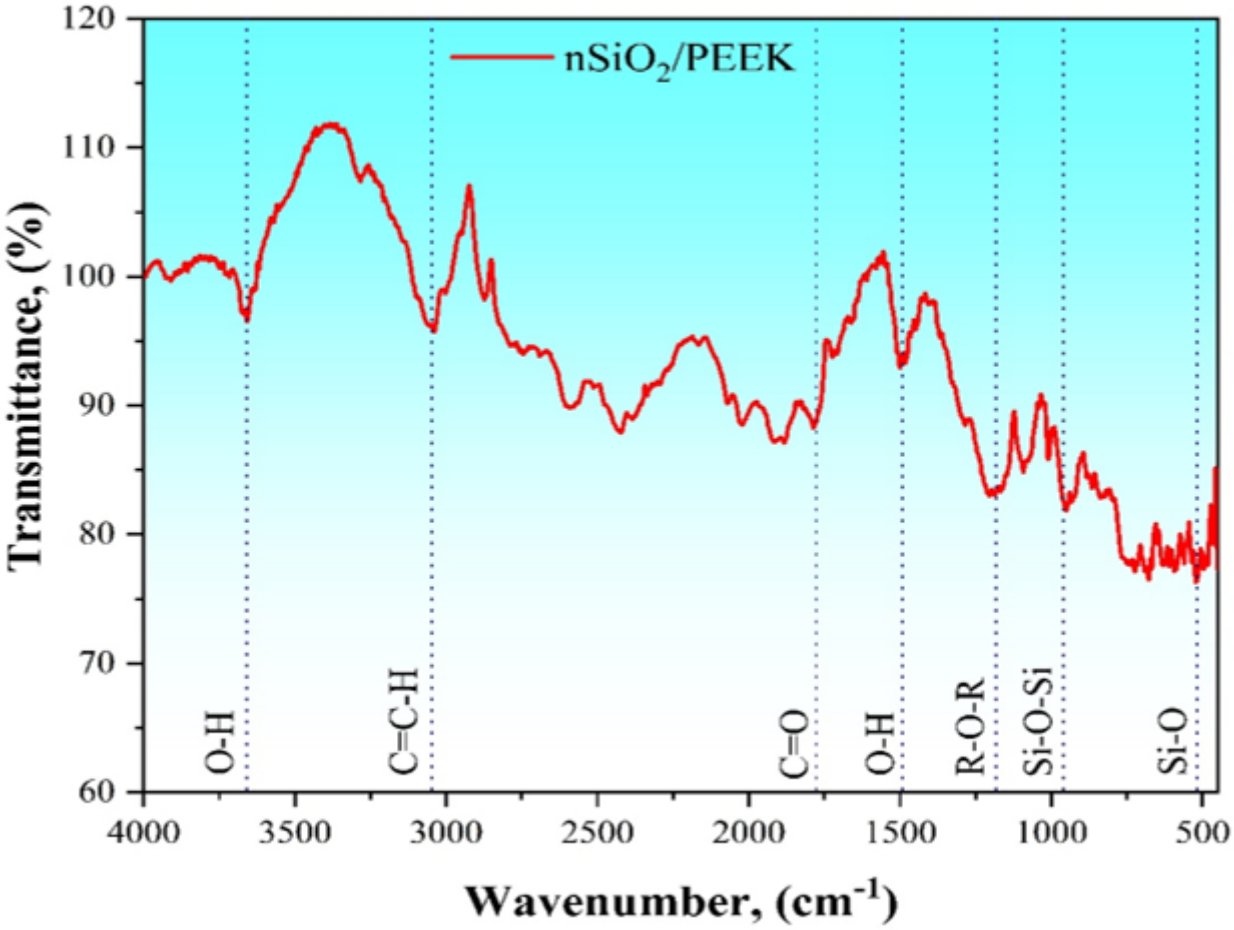

Figure 5

FTIR spectrum of developed $nSiO_2$@PEEK polymer composite

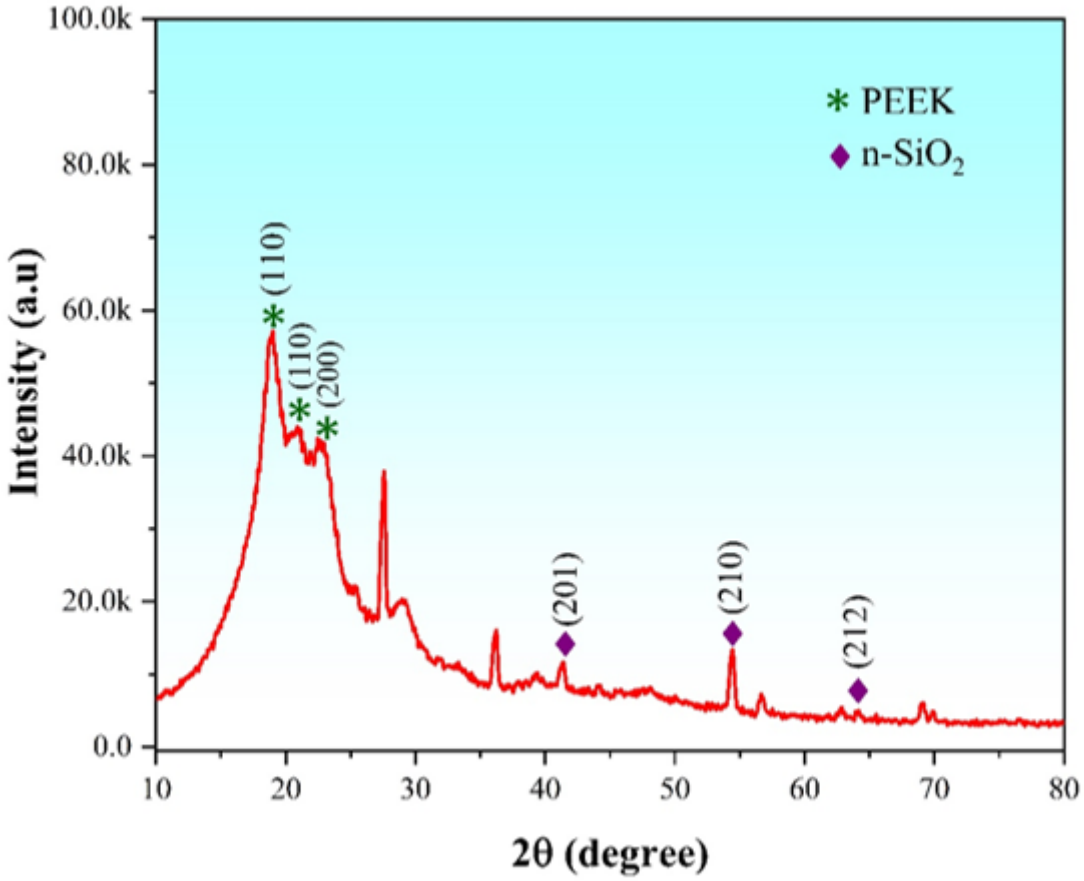

Figure 6

XRD pattern of nSiO2@PEEK polymer composite

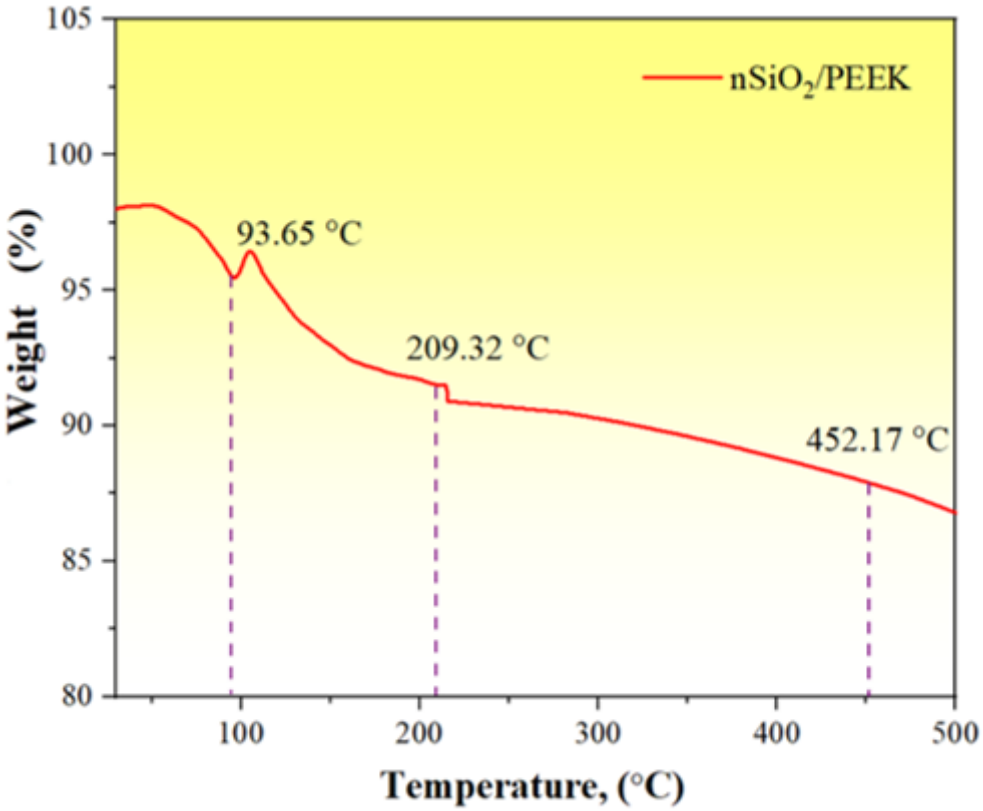

Figure 7

TGA thermogram for $nSiO_2$@PEEK polymer composite

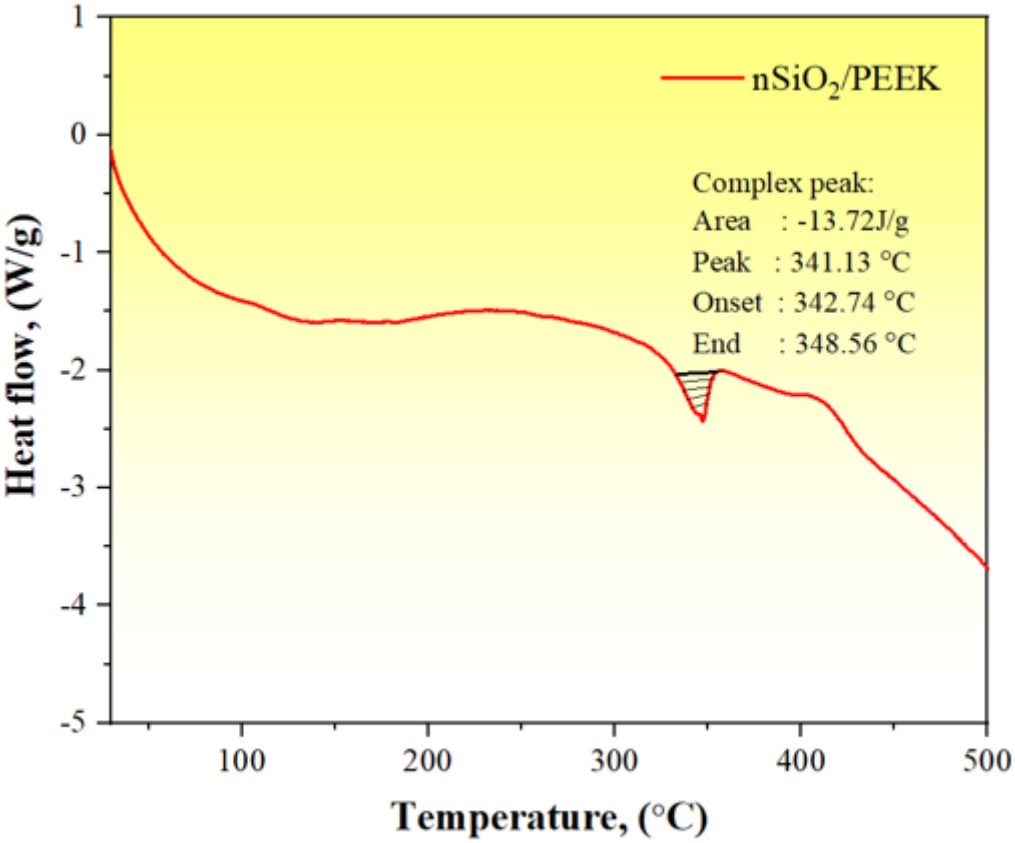

Figure 8

DSC curve for $nSiO_2$@PEEK polymer composite

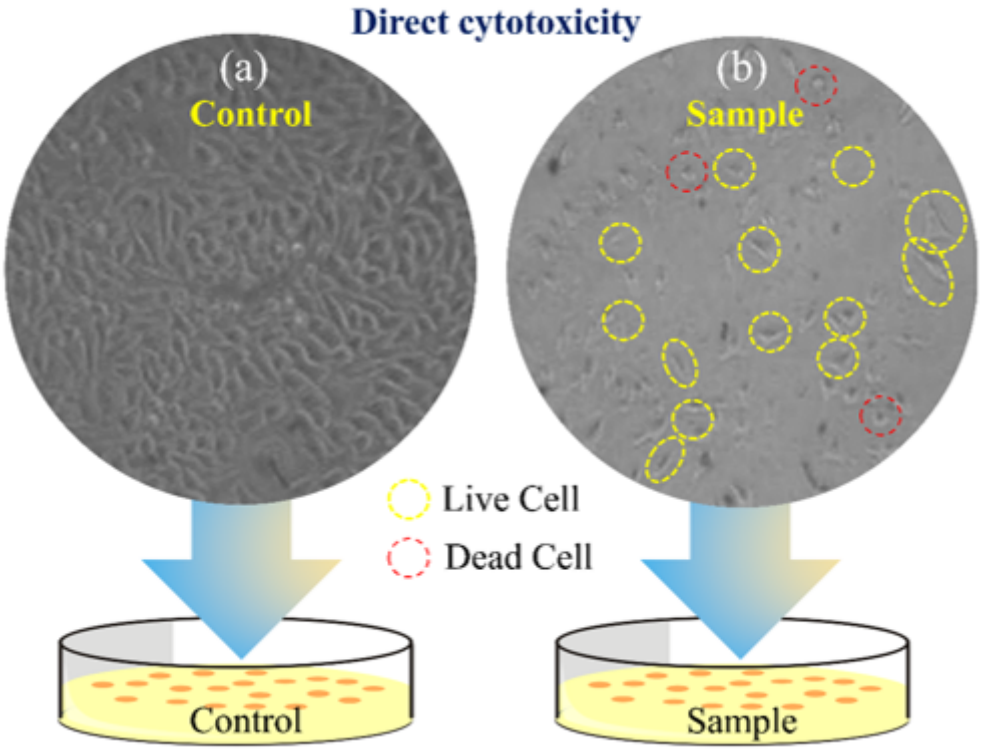

Figure 9

Observation of living and non-living cells using phase-contrast microscopic; control (a) and sample (b) by direct cytotoxicity method.

Figure 10

Observation of living and non-living cells using phase-contrast microscopic; control (a) and sample (b) by indirect cytotoxicity method.

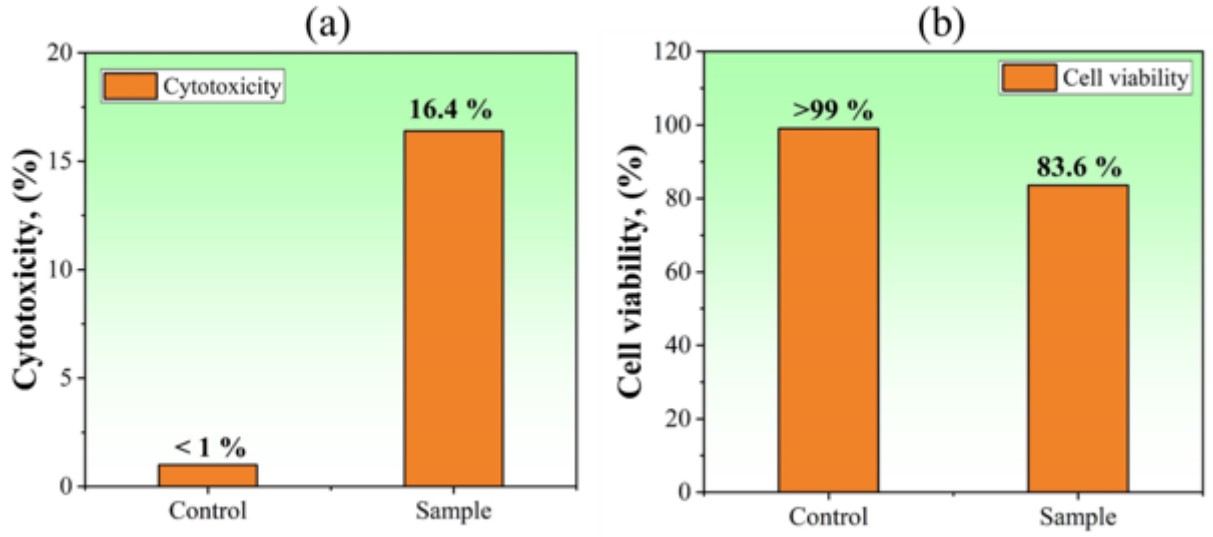

Figure 11

(a) Percentage of cytotoxicity and (b) cell viability of developed composite material

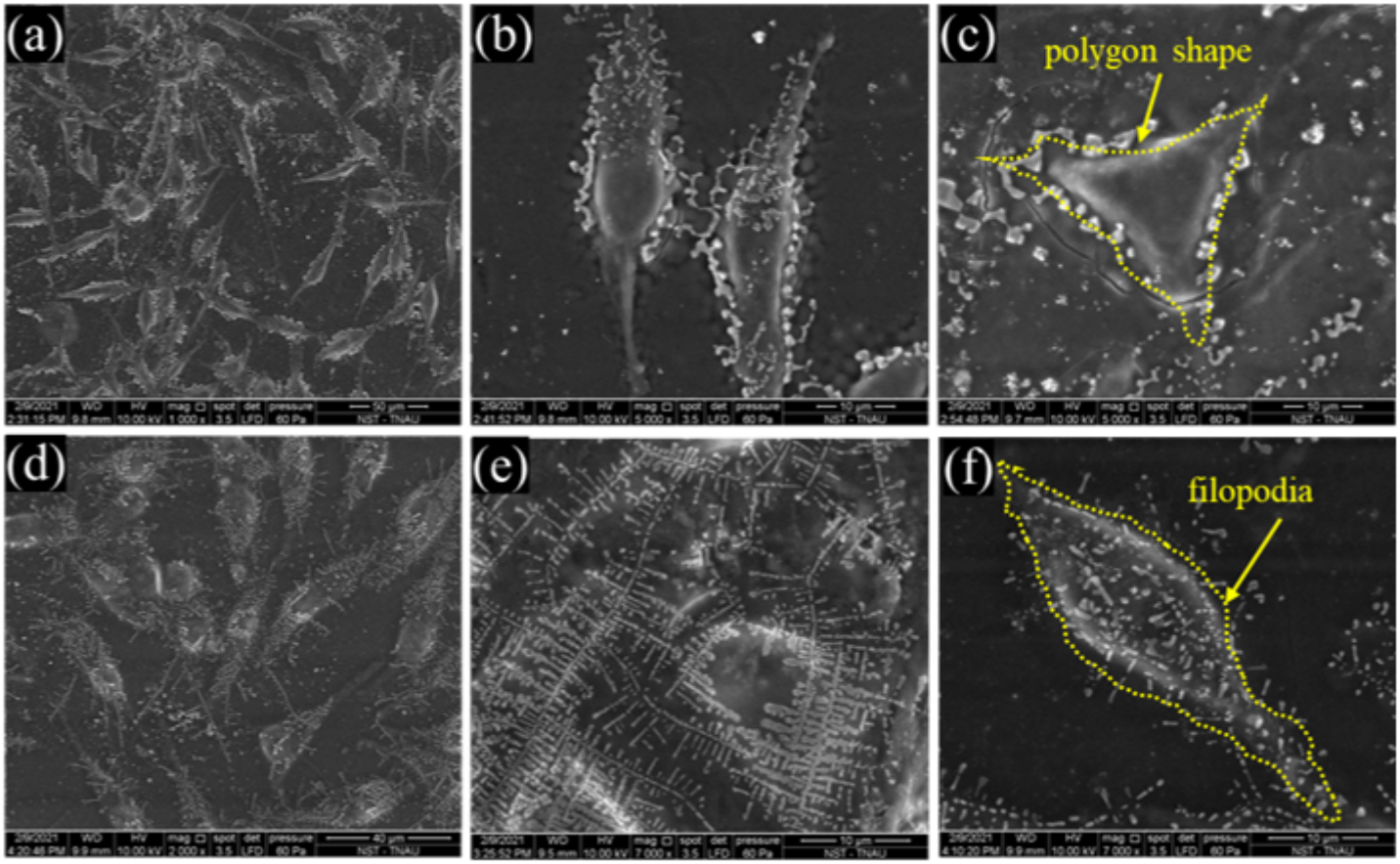

Figure 12

MG-63 cell attachment regarding cell growth and proliferation of adhered cells morphologies at different locations (a-f) by SEM.